Evaluation of a Traditional Scaling Method for Pediatric Head-Neck Responses in a Simulated Frontal Impact

Yun-Seok Kang, Rosalie Connell, David Stark, Julie Mansfield, John H. Bolte IV

Abstract Scaled biomechanical corridors are derived from scaled 50th percentile male data, which have been shown to be insufficient in capturing pediatric biomechanical responses. The objective of this study is to collect biomechanical responses of a 15-year-old (15YO) head-neck complex to be compared to the corridors obtained through a traditional scaling method. A mini-sled was used, as in previous tests with head-neck complexes of adult male post-mortem human subjects (PMHS), to conduct dynamic testing on a 15YO PMHS head-neck complex. Results were compared to those developed from the previously collected scaled adult data to assess a traditional scaling technique (e.g. Irwin and Mertz). The traditional scaling technique mostly underestimated several pediatric responses when compared to 15YO PMHS head-neck responses in a simulated frontal impact. Comparing true pediatric head-neck biomechanical responses to those derived from the traditional scaling method will provide insight into the need for further refinement of scaling techniques, which will lead to accurate biomechanical corridors and will enhance injury prevention for the pediatric population.

Keywords Cervical spine, pediatric, head-neck complex, scale factor, traditional scaling technique.

I. INTRODUCTION

Motor vehicle collisions (MVCs) are a global burden, resulting in 1.3 million deaths each year and remaining the leading cause of death for children and young adults aged 5–19 years in 2022 [1,2]. Within the pediatric population, MVCs are also the leading cause of spinal injury [3,4]. Although the instance of spinal injuries is relatively low, cervical spinal injuries, specifically those associated with frontal impact MVCs, are some of the most severe injuries sustained by pediatric occupants [5-7]. Injury to the upper cervical spine is particularly devastating and more common in pediatric populations due to children's anatomical specificities. The etiology of these injuries is related to younger children's higher fulcrum of motion, underdeveloped vertebrae, lack of ossification, flexible ligaments and shallow facet joints, all of which contribute to injury occurrence above the C2 level for children under 8 years old [8-10]. Between the ages of approximately 9 and 12 years, lower cervical spine injuries become more prevalent with anatomical maturation [3-5]. The prevalence of pediatric cervical spinal injury is highest in pre-adolescent and adolescent groups (8-18 years old) when compared to younger pediatric and adult populations [4][11-13]. Despite injuries transitioning to the lower neck, which resemble those sustained by adults, injury outcomes and occurrences within this adolescent group are still unique to the pediatric population, as evident through injury outcomes such as spinal cord injury without radiographic abnormality (SCIWORA) [13] and differences in injury frequency patterns [5].

Given the importance of protecting occupants against such injuries, there remains much to be understood about the occurrence of cervical spine injuries for the pediatric population. Several studies have been conducted on adult post-mortem human subjects (PMHS) to understand cervical spine injuries under dynamic frontal loading environments such as would be experienced during a MVC [14-16]. However, the scarcity of pediatric PMHS means there is limited understanding of pediatric cervical spine biomechanical responses in such dynamic environments. Previous work has investigated the mechanical properties of the pediatric cervical spine via tests with isolated cervical spines and spinal functional units [17,18]. While enlightening, these tests did not capture the soft tissue's viscoelastic responses, as would be observed within the full head-neck complex. Other work that was able to account for viscoelasticity focused primarily on quasi-static testing under a single loading direction, which determined the cervical stiffness for age groups between 2–4 and 6–12 years [19]. Today, analyses for the

Y. Kang, PhD, (e-mail: yunseok.kang@osumc.edu; tel: +1 614 366 7584; fax: +1 614 292 7659) is an Associate Professor and R. Connell, D. Stark, PhD, J. Mansfield, PhD, and J. Bolte, PhD, are student and faculty in the Injury Biomechanics Research Center at the Ohio State University in Columbus, OH, USA.

dynamic responses of pediatric head and neck complexes are still highly dependent on animal surrogates [20] or computational models [21,22], despite each having their own unique limitations.

Pediatric injury prevention techniques have therefore been developed and assessed based on the corridors derived from geometrically scaled data from the 50th percentile male [23]. These scaled corridors have been utilised extensively to develop pediatric anthropomorphic test devices (ATDs) and computational models, although evidence has shown limitations in such methods to capture the true pediatric response [24]. Further, when comparing biomechanical responses of adults and pediatric living human subjects within sub-injurious thresholds, there are stark differences between true pediatric responses and scaled adult data [25,26]. Evident biomechanical differences between adult and pediatric cervical spines highlight the critical importance of specialised investigations into the pediatric population.

With this, there remains a lack of understanding of the biomechanical response of the pediatric spine. No previous studies have subjected pediatric and adult PMHS to the same simulated frontal impact conditions at injurious levels and compared them directly to evaluate how the true pediatric response compares to those derived from scaled corridors. The objective of this study is to provide head and neck kinematics and kinetics of a 15YO PMHS in a frontal impact and to compare these data to corridors established from traditionally scaled adult data collected under the same testing conditions. This study will be the first to quantify the dynamic responses of the pediatric cervical head and neck complex alone and to evaluate the accuracy of currently used scaling methods for this important anatomical region. The results can be utilised to refine scaling techniques and to develop new biomechanical targets to validate pediatric ATDs and computational human body models in the future.

II. METHODS

Post-mortem Human Subjects (PMHS) Information

A pediatric male PMHS (15YO) was available through The Ohio State University Body Donation Program. This study was carefully reviewed by The Ohio State University Body Donation Program Advisory Committee, our internal ethics committee for the use of PMHS in research. The research protocol was deemed to be an ethical utilisation of the special donation, with particular consideration for the critical need for pediatric biomechanical data and the valuable contribution the data generated can provide to injury prevention efforts, providing extensive societal benefits. Characteristics for the pediatric PMHS and previously tested adult PMHS are provided in Table I, and additional information can be found in [15]. PMHS head and neck anthropometry and weight measures are also presented in the Appendix, in Table AI. A computed tomography (CT) scan was taken to ensure there were no abnormalities in the cervical and upper thoracic spine. The head and neck complex, including the upper thoracic region, were dissected using the same procedure outlined in the previous study [14].

Experimental Setup

The same mini-sled used in the previous adult PMHS study [14,15] was also utilised in this study to simulate a frontal impact scenario at a nominal velocity of 14 km/h. This nominal velocity was the same as the previous adult PMHS mini-sled study, which was based on T1 x-acceleration from a full body frontal PMHS test conducted by Pintar *et al.* [27]. Figure 1 shows the general mini-sled testing configuration, instrumentation, and sled input direction from a previous adult PMHS test, which was consistent with the experimental setup for the pediatric PMHS. An elliptical ring was attached to upper thoracic structures, including the clavicles, 1st ribs, muscles, and surrounding skin, as shown in Fig. 1A. The elliptical ring was attached to turnbuckles (Fig. 1B) in line with uniaxial load cells (Fig. 1C) that were fixed to the mini sled to measure passive muscle forces during the event. Initial neck pre-load was adjusted to approximately 55 N, which was determined by applying a scale factor (0.55 from [28] to the adult neck pre-load setup (~100N from [14]), by tuning the turnbuckles. The 3rd thoracic vertebra was affixed within a potting cup using the same potting material used for the adult PMHS tests (Bondo Corporation, Atlanta, GA, USA). As shown in Fig. 1, the potting cup (Fig. 1D) was fixed in line with a six-axis load cell (Fig. 1E) (Humanetics Innovation Solutions, Farmington Hills, MI, USA) to measure lower neck forces and moments. For the PMHS kinematics, accelerometers and angular rate sensor arrays were installed at the head (6aω), C3 (3aω) and C6 (3aω), as shown in Fig. 1F and Fig. 1G. The head was suspended by a solenoid release system (Fig. 1H), which was activated right before the mini sled started motion. Further information on fixture setup, PMHS preparation and instrumentation can be found in [14,15].

TABLE I
PMHS INFORMATION
PED: PEDIATRIC PMHS, ADT: ADULT PMHS

	Age (yrs)	Sex	Height (cm)	Weight (kg)
PED	15	Male	170.5	52.6
ADT1	67	Male	184.5	71.0
ADT2	57	Male	175.0	64.0
ADT3	54	Male	175.3	74.1
ADT4	25	Male	177.8	73.4
ADT5	40	Male	175.3	67.0
ADT50M Mean (SD)	49 (16)	Male	177.6 (4.0)	69.9 (4.3)

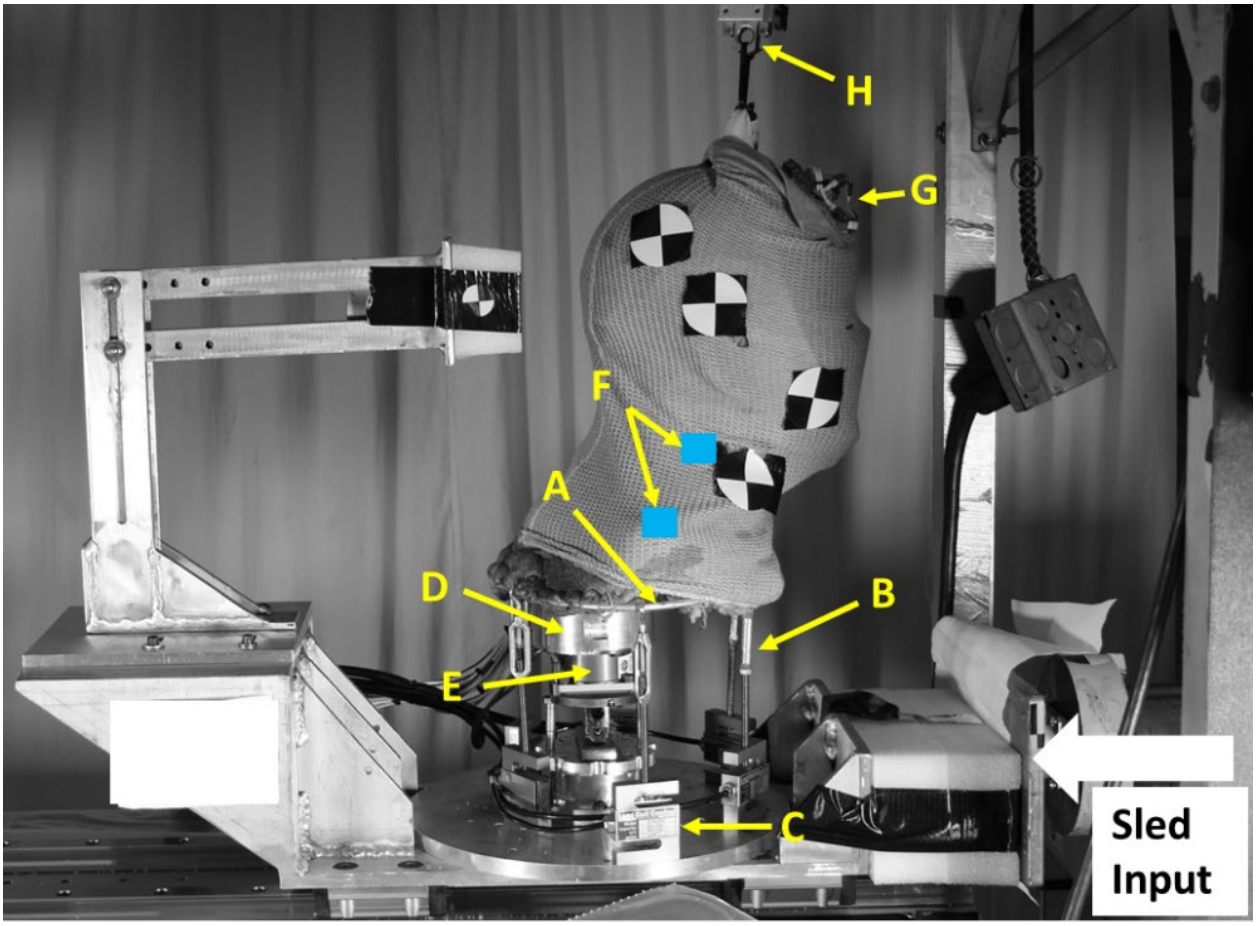

Fig. 1. Mini-sled general set-up and instrumentation in an adult PMHS test.
A: custom-sized elliptical ring, B: turnbuckles for initial muscle tension, C: uniaxial load cells, D: potting cup at T3, E: six-axis load cell, F: motion block at C3 and C6, G: head 6aω, H: head release system.

Traditional Scaling Method

A traditional scaling method (TSM) proposed by [29] and further studies by Mertz *et al.* [28] [30] were used in this study. Relevant anthropometric measures used to determine scale factors for the 10YO demographic proposed in the TSM are provided in Table II. These data were utilised as the 10YO is the closest available set of scaling data comparable to the 15YO pediatric PMHS subject from this study. Failure stresses of the calcaneal tendon [31] and anthropometric measures served as the basis for calculations of the scale factors for the acceleration, time, force and moment in the TSM. Equations (1)–(4) list the formulas for TSM scale factors previously proposed [28][30]

for the experimental outcomes. The head acceleration scale factor can be calculated using a failure stress scale factor and a length scale factor:

$$\lambda_a = \lambda_\sigma / \lambda_L \quad (1)$$

where λ_a is a head acceleration scale factor, λ_σ represents a failure stress scale factor, and λ_L is a length scale factor calculated using a sum of head circumference (C), width (W), and depth (D).

The equal linear velocity assumption from TSM was also applied to the angular velocity scale factor (i.e. both linear and angular velocity scale factors were at unity).

For the neck force and moment scale factors, a failure stress scale factor and a neck circumference scale factor were used in Equations (2) and (3):

$$\lambda_F = \lambda_\sigma \times \lambda_C^2 \quad (2)$$

where λ_F is a neck force scale factor, λ_C represents neck circumference.

$$\lambda_M = \lambda_\sigma \times \lambda_C^3 \quad (3)$$

where λ_M is neck moment scale factor.

The angle scale factor was determined using the erect sitting height scale factor and mass scale factor:

$$\lambda_\theta = \lambda_z / \lambda_x \quad (4)$$

where λ_θ is a rotation (or angle) scale factor, λ_z represents an erect sitting height scale factor, $\lambda_x = \lambda_m / \lambda_z$, where λ_m is a total body mass scale factor. The neck angle scale factor was also applied to the head rotation.

Since head and neck anthropometries for both pediatric and adult PMHS were measured in the current and previous study [15], scale factors specific for the 15YO PMHS were also calculated with TSM by utilising anthropometric measures from adult and pediatric PMHS subjected to the current testing conditions. The measures referenced for these specific scaling factors are provided in Table AI, aside from the failure stress for 15YO, which was unknown. Ten-year-old failure stress was applied to the 15YO scaling equations assuming that the difference in failure stress between 10YO and 15YO is minimal. This assumption is supported by the original source for failure stresses used in the TSM, which reports mechanical properties over age by decade, therefore the values reported for 10YO would also be applicable for 15YO [31]. To generate scaled corridors for 10YO and 15YO, the scale factors provided in Table II were applied to the adult PMHS corridors (ATD50M mean ± one standard deviation) from the previous study [15].

Data Collection, Reduction and Processing

Pediatric PMHS data were recorded at the sampling frequency of 20,000 Hz using the same data acquisition system (G5, DTS, Seal Beach, CA, USA) used in the previous adult PMHS study. All data were zeroed and filtered at the same cut-off frequencies used in the previous adult PMHS studies (Table AII). Processing methods for the pediatric PMHS kinematic and kinetic data in the current study were consistent with previous adult PMHS studies [14,15]. In brief, the head 6aω data were transformed to the estimated head centre of gravity (CG). The pediatric head CG was determined using CT images [32], while the adult PMHS head CG was measured physically [14]. Pediatric PMHS head mass (3.13 kg) was measured during post-test dissection and was used to determine upper neck forces using an inverse dynamics technique [14]. The C3 and C6 motion block data were transformed into an anatomical coordinate system following SAEJ211 convention, as used in adult PMHS studies [15]. The lower neck loads were calculated using both the six-axis load cell at T3 and the muscle tension load cells [14]. Results with respect to the local coordinate system are reported as x-, y- and z-axis, whereas sled reference frames are reported as X-, Y- and Z-axis. More detailed information for kinematics and kinetic analyses, as well as anatomical coordinate systems for the head and neck complex, was provided in the previous adult PMHS studies [14,15].

To quantify differences in responses between the scaled corridor and the pediatric PMHS, an NHTSA BioRank method was used [33]. A BioRank Score (BRS) and phase difference (P) between the pediatric response and the scaled corridor mean were determined for quantitative assessment. A BRS score of 1 means that the pediatric

PMHS response is one standard deviation away from the scaled corridor means, and a lower score suggests stronger agreement between the responses. Peak errors between the pediatric responses (true value) and scaled corridor mean responses (estimated value) were also calculated. Peak errors with a negative sign mean that the scaled corridor mean responses were *under*estimated as compared to the pediatric responses, while the positive sign means *over*estimated scaled responses.

TABLE II
SCALE FACTORS AND RELEVANT ANTHROPOMETRIC MEASURES

	50th Male	10YO	Mean ADT50M	15YO
Calcaneal tendon (MPa)	54.9	53.8	N/A	N/A
Stress scale factor, λ_σ	1.00	0.98	N/A	N/A
Total body mass (kg)	78.2	32.4	69.9	52.6
Mass scale factor, λ_{m}	1.00	0.41	1.00	0.75
Erect sitting height (cm)	90.7	71.9	92.1	83.5
Height scale factor, λ_{Z}	1.00	0.79	1.00	0.91
Head C+W+D (cm)*	92.5	86.1	91.7	88.1
Head length scale factor, λ_L	1.00	0.93	1.00	0.96
Head acceleration scale factor, $\lambda_a = \lambda_\sigma/\lambda_L$	1.00	1.05	1.00	1.02
Head velocity scale factor, $\lambda_{\mathrm{V}} = 1$	1.00	1.00	1.00	1.00
Neck circumference (cm)	38.3	28.7	38.4	34.0
Neck circumference scale factor, λ_{C}	1.00	0.75	1.00	0.89
Neck force scale factor, $\lambda_F=\lambda_\sigma\times\lambda_C^2$	1.00	0.55	1.00	0.77
Neck moment scale factor, $\lambda_M=\lambda_\sigma\times\ \lambda_C^3$	1.00	0.41	1.00	0.68
Angle scale factor, $\lambda_\theta=\lambda_z/\lambda_x$	1.00	0.91	1.00	1.00

*C: circumference, W: width, D: depth

III. RESULTS

The pediatric PMHS responses were plotted against two scaled corridors (scaled 10YO corridor and scaled 15YO corridor). Figure 2 shows generic plots to demonstrate how all plots will be provided throughout the Results section. A red solid line with a red-filled area and a blue solid line with a blue-filled area represent a mean curve with the upper and lower boundary of the scaled corridors (mean ± one standard deviation) for 10YO and 15YO, respectively. BRS and P are provided in the plots (scaled 10YO corridor vs. pediatric response shown in red and scaled 15YO corridor vs. pediatric response shown in blue). Figures 2(a) and 2(b) show two scaled corridors with and without overlap, respectively. Small differences in scale factors between 10YO and 15YO result in large overlap between both corridors (purple-coloured shaded area), as shown in Fig. 2(b).

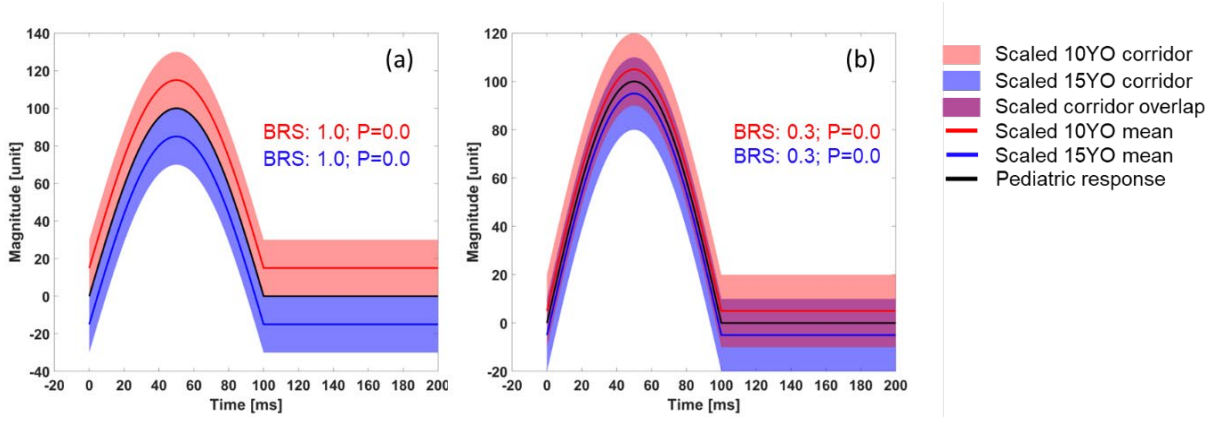

Fig. 2. Generic result examples illustrating (a) no overlap between red and blue; (b) overlap shown in purple

Figure 3 shows the head kinematics of the pediatric PMHS compared to the scaled corridors for 10YO and 15YO, respectively. Due to minimal differences in head kinematic scale factors between 10YO and 15YO (Table II), the scaled corridors exhibit a large overlap (purple colour). Overall, pediatric BRS scores against 15YO scaled corridors were larger than those for 10YO scaled corridors with the exception of the angular velocity about the y-axis. A similar trend was found in the peak values and peak errors (Table III). BRS scores for the head acceleration in the z-direction, angular velocity about the y-axis, and rotation about Y-axis ranged from 1.0 to 1.23 for both scaled 10YO and 15YO corridors, while those for the head acceleration in the x-direction and displacements in the X- and Z-directions were less than 1.0. For the percent peak errors of the head kinematics, the largest error was found in the head rotation (42.6%) for the scaled 15YO, while the smallest error was from the head displacement in the X-direction for the scaled 10YO (2.6%), shown in Table III. Negative peak errors were found in the scaled head acceleration and angular velocity in Table III, implying that the TSM resulted in underestimated responses as compared to the pediatric responses. However, the opposite trend was found in the head rotation and displacement, exhibiting overestimated positive peak errors (Table III). It should be noted that the pediatric head kinematics were delayed as compared to the scaled corridors due to a head lag (i.e. the head tended to stay in place while the lower neck and the mini sled started moving), likely due to compliance of the pediatric neck.

The upper neck forces in the x- and z-directions (Fx and Fz) are shown in Fig. 4(a) and (b), respectively. BRS scores and percent peak errors for the scaled 10YO (2.06 and 1.96 for Fx and Fz; |percent peak errors| > 50%) were greater than those for the scaled 15YO (0.94 and 1.32 for Fx and Fz; |percent peak errors| > 30%), shown in Fig. 4 and Table III. The TSM resulted in underestimated scaled upper neck forces (e.g. peak percent errors were negative) as compared to the pediatric responses. The head lag was also observed in upper neck forces in Fig. 4.

Figure 5 shows rotations about the Y-axis at the 3rd and 6th cervical vertebrae (C3 and C6). For the C3 rotation, the BRS scores and percent peak error were 1.11 and 11.6% for the scaled 10YO and 0.45 and 2.8% for the scaled 15YO. The C6 rotations exhibited a larger discrepancy between the pediatric response and scaled corridors, which resulted in BRS greater than 1.0 (1.73 for scaled 10YO, 1.32 for scaled 15YO) and over 20% errors (32.2% for scaled 10YO, 25.5% for scaled 15YO).

The lower neck loads are shown in Fig. 6. The BRS scores for the Fx and Fz were greater than 1.00 in both scaled 10YO (1.53 for Fx, 1.93 for Fz) and 15YO (1.37 for Fx, 1.14 for Fz) corridors, while those for the moment about the y-axis (My) were 1.00 for the scaled 10YO and 0.70 for the scaled 15YO. The percent peak errors for both Fx and Fz were greater than 35%, except the Fx for the scaled 10YO (1.6%), while those for My were 48.6% for the scaled 10YO and 14.7% for the scaled 15YO. It should be noted that the scaled 15YO Fx overestimated the scaled pediatric responses, while the peak mean values for 10YO was close to the peak value from the pediatric PMHS (1.6% peak error). The scaled responses for both 10YO and 15YO were underestimated, as shown in Fig. 6(b) and (c). The head lag also affected the phase differences in the lower neck loads between the pediatric and adult PMHS.

The pediatric PMHS responses overlaid with unscaled adult PMHS corridors were provided in Appendix B (Figs B1–B4). Peak mean values from the unscaled adult PMHS are also presented in Table III, with good agreement (|percent error| < 20%) highlighted in green, moderate agreement (20% < |percent error| < 30%) in orange, and poor agreement (|percent error| > 30%) in red.

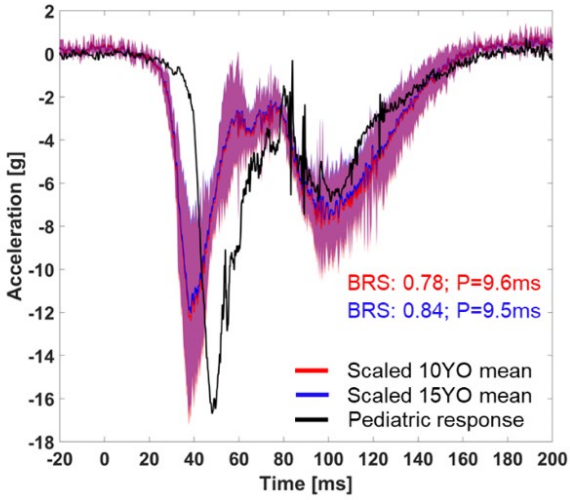

(a) Acceleration in x-direction.

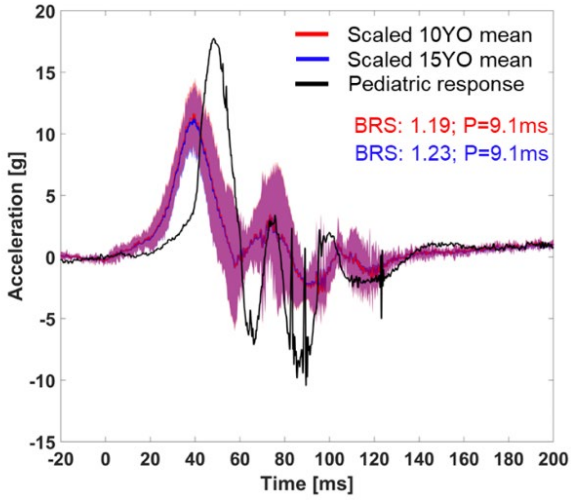

(b) Acceleration in z-direction.

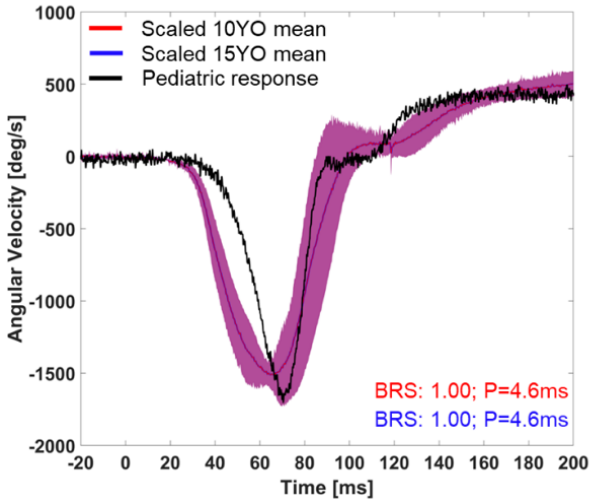

(c) Angular velocity about y-axis.

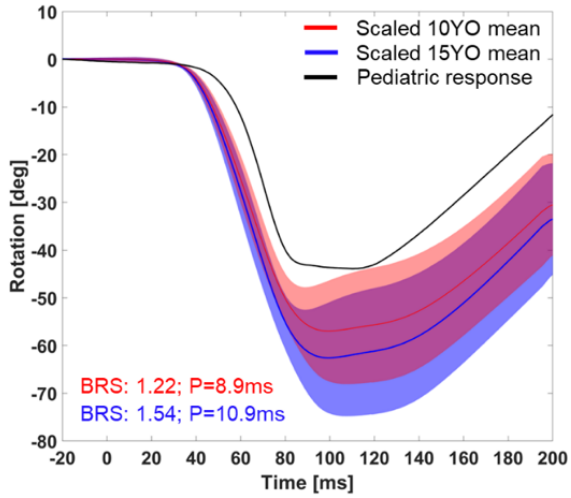

(d) Rotation about Y-axis.

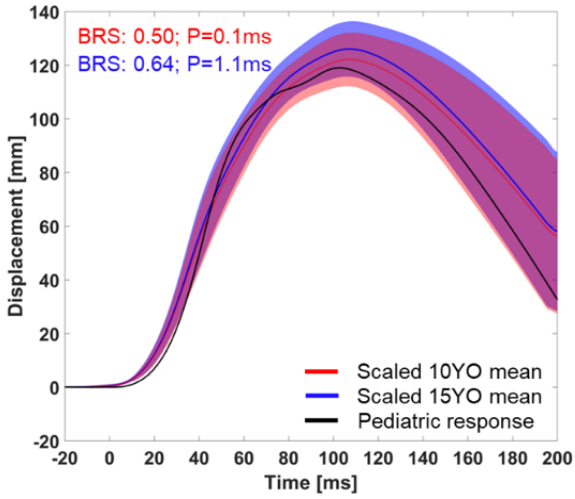

(e) Displacement in X-direction.

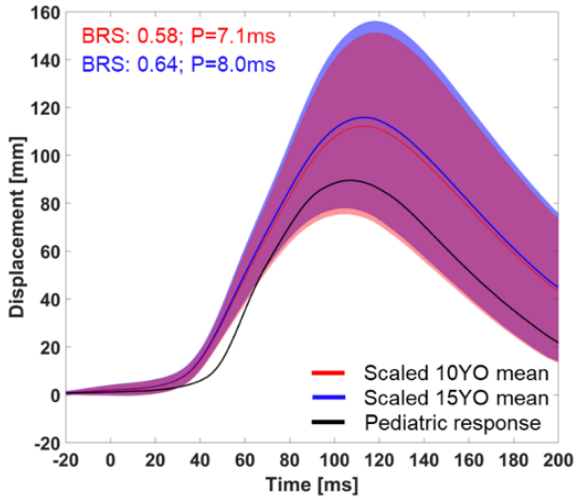

(f) Displacement in Z-direction.

Fig. 3. Head kinematics comparison of pediatric PMHS (black) to scaled 10YO corridors (red) and scaled 15YO corridors (blue).

TABLE III
PEAK VALUE AND PERCENT ERROR
NEGATIVE PERCENT ERROR MEANS TSM UNDERESTIMATED SCALED MEAN

		Peak value				Percent error (%)		
		Adult (N=5)	Scaled 10YO	Scaled 15YO	**PED (N=1)**	Adult (N=5)	Scaled 10YO	Scaled 15YO
Head Kinematics	Acceleration in x-direction (g)	-11.8	-12.4	-12.0	**-16.7**	-29.4	-25.8	-27.9
	Acceleration in z-direction (g)	11.1	11.7	11.3	**17.8**	-37.5	-34.4	-36.3
	Angular velocity about y-axis (deg/s)	-1512.5	-1512.5	-1512.5	**-1706.0**	-11.3	-11.3	-11.3
	Rotation about Y-axis (deg)	-62.6	-57.0	-62.6	**-43.9**	42.7	29.8	42.6
	Displacement in X-direction (mm)	131.3	122.1	126.1	**119.0**	10.3	2.6	5.9
	Displacement in Z-direction (mm)	120.7	112.2	115.8	**89.6**	34.8	25.3	29.3
Upper Neck Force	Force in x-direction (N)	-455.8	-250.7	-351.0	**-526.7**	-13.5	-52.4	-33.4
	Force in z-direction (N)	424.6	233.5	327.0	**541.3**	-21.6	-56.9	-39.6
C3 and C6 Rotation	C3 rotation about Y-axis (deg)	-57.9	-52.7	-57.9	**-59.6**	-2.8	-11.6	-2.8
	C6 rotation about Y-axis (deg)	-31.5	-28.6	-31.5	**-42.2**	-25.4	-32.2	-25.5
Lower Neck Load	Force in x-direction (N)	-654.9	-360.2	-504.2	**-366.1**	78.9	-1.6	37.7
	Force in z-direction (N)	468.0	257.4	360.3	**615.5**	-24.0	-58.2	-41.5
	Moment about y-axis (Nm)	98.9	40.5	67.2	**78.8**	25.5	-48.6	-14.7

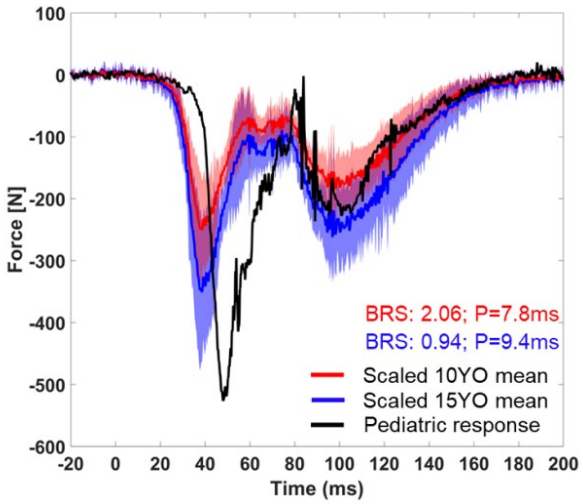

(a) Force in x-direction.

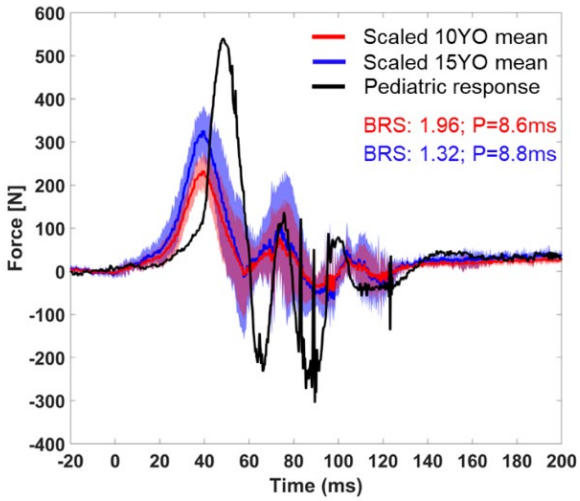

(b) Force in z-direction.

Fig. 4. Upper neck load comparison of pediatric PMHS (black) to scaled 10YO corridors (red) and scaled 15YO corridors (blue).

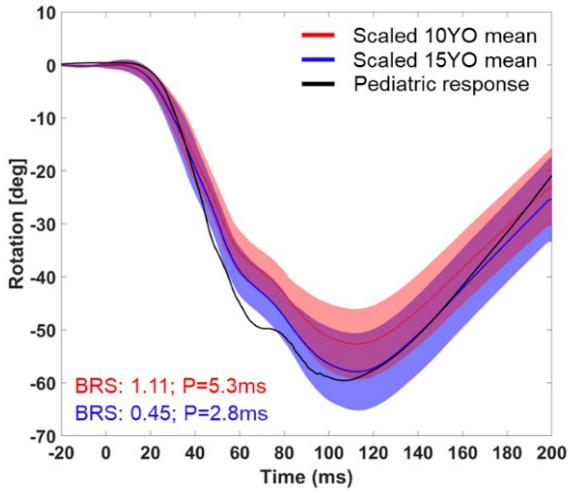

(a) C3 rotation about Y-axis.

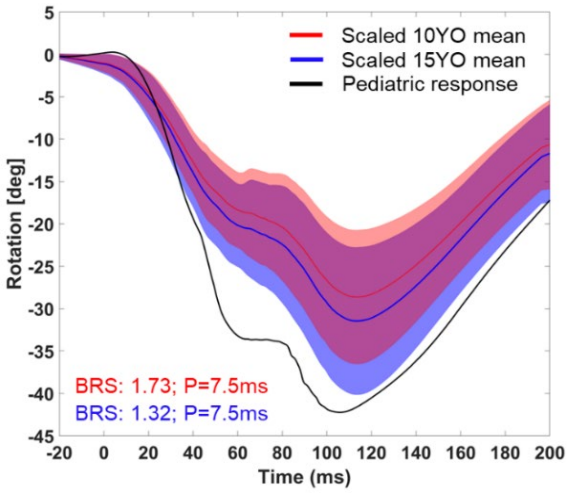

(b) C6 rotation about Y-axis.

Fig. 5. C3 and C6 rotation comparison of pediatric PMHS (black) to scaled 10YO corridors (red) and scaled 15YO corridors (blue).

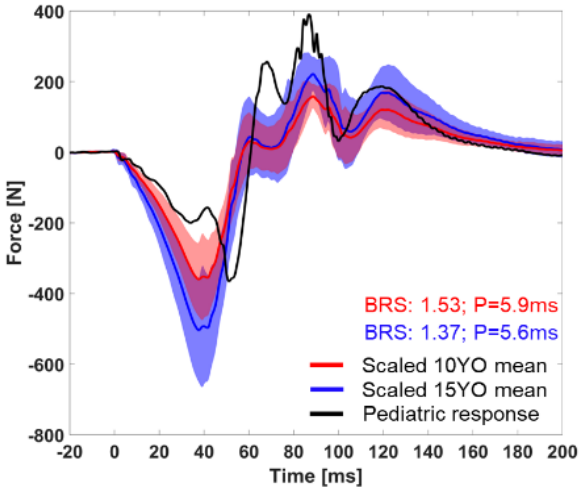

(a) Force in x-direction.

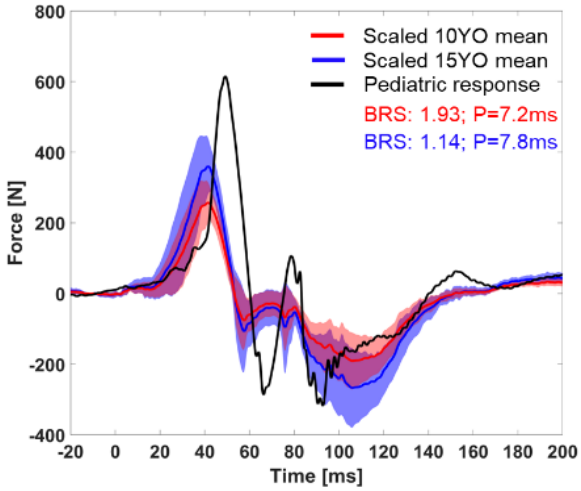

(b) Force in z-direction.

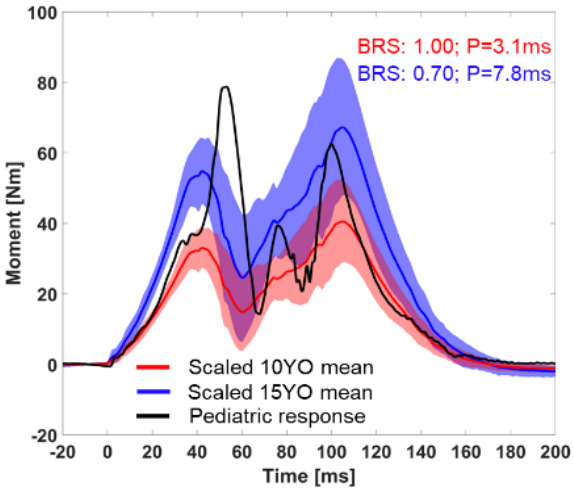

(c) Moment about y-axis.

Fig. 6. Lower neck load comparison of pediatric PMHS (black) to scaled 10YO corridors (red) and scaled 15YO corridors (blue).

IV. DISCUSSION

In this study, biomechanical responses of a 15YO head-neck complex mounted to a mini sled were investigated in a simulated frontal impact condition and compared to the scaled 10YO and 15YO corridors generated using the TSM. The TSM resulted in underestimated scaled corridors for the head acceleration and angular velocity, cervical spine rotations, and loads at the upper and lower neck (except the lower neck Fx). In contrast, the head global displacements and rotation were overestimated.

Traditional Scaling Method

In TSM, the head acceleration scale factor was dependent on the stress scale factor (λ_σ) and head length scale factor (λ_L), which were calculated using a sum of the head circumference, width and depth [29]. Given the 15YO stress scale factor was assumed to be the same as the 10YO stress scale factor in the current study, the difference in head acceleration scale factors between 10YO and 15YO was dominated by the head length scale factor shown in Table II. The TSM failed to estimate the pediatric responses, resulting in underestimated head acceleration in both x- and z-directions (absolute errors ranged from 25.8% to 36.3% in Table III). A similar trend was observed in the upper neck forces. It should be noted that upper neck forces were calculated using an inverse dynamics approach (upper neck forces = head mass x head acceleration), which means that the upper neck forces were scaled by head mass from the head acceleration. However, the neck force scale factor was a function of the stress scale factor (λ_σ) and square of the neck circumference scale factor ($\lambda_C{}^2$). The neck force scale factor had to be sensitive to the neck circumference scale factor. The most considerable discrepancy between the scaled corridors and the pediatric PMHS responses was found in the upper neck force (over 50% error in scaled 10YO and over 30% error in scaled 15YO). The upper neck force scale factors may be related to head inertial properties instead of neck size.

The lower neck Fz showed a similar trend as the upper neck forces, resulting in an absolute error of over 40% (Table III). Interestingly, the peak lower neck Fx of the pediatric PMHS was consistent with the peak mean scaled 10YO Fx, resulting in an absolute error of 1.6%. However, the discrepancy in time history between the scaled 10YO and the pediatric PMHS was observed in Fig. 5(a) (BRS = 1.53). Unlike the 10YO lower neck Fx, the TSM generated overestimated Fx for scaled 15YO (absolute error: 37.7%). The scaled 15YO mean neck moment was closer to the pediatric neck moment than the 10YO shown in Fig. 5(c) and Table III. However, the TSM underestimated the neck moment for the 10YO in both time history and peak value evaluation. The lower neck moment scale factor was determined using the stress scale factor (λ_σ) and power of neck circumference scale factor ($\lambda_C{}^3$). The power of the neck circumference scale factor and the stress scale factor could be a dominant error source for the moment scale factor. As a result, both force and moment scale factors are dominated by the stress scale factor (λ_σ), and the neck circumference scale factor ($\lambda_C{}^2$ and $\lambda_C{}^3$) was unable to predict the pediatric PMHS upper and lower neck loads.

Unlike the head acceleration and loads at the upper and lower neck (except lower neck Fx), the TSM overestimated the head displacement and the head rotation shown in Fig. 5(d)–(f) and Table III. Head displacement was scaled using the head length scale factor (λ_L) and the head rotation scale factor was assumed to be the same as the neck rotation scale factor, which was dependent on the erect height scale factor and the total body mass scale factor. Lopez-Valdes *et al*. (2012) showed an underestimation of the scaled head excursion using the TSM compared to pediatric volunteers' responses [24]. This inconsistency with the current study might be due to differences in speed and testing specimen (volunteer vs. PMHS). Additionally, the current data were not normalised to seated height of the subject, as was done in previous work [24][26] which may have resulted in similar underestimations by the corridors. An opposite trend was found in C3 and C6 rotations (i.e. the TSM underestimated the scaled C3 and C6 rotations). The directionality of the errors from the TSM was not systematic, given that both underestimated and overestimated scaled outcomes resulted from the current study. Regardless, based on the results from the current study, the TSM was unable to estimate the pediatric PMHS responses.

Many studies have investigated scaling methods for pediatric head and neck responses using different engineering theories and material and mechanical properties of the human body regions [23][24][30][34]. The most popular method that has been used for designing, fabricating and evaluating current ATDs and HBMs was the TSM developed by Irwin, Mertz and colleagues. Irwin and Mertz (1997) and Mertz *et al*. (2001) developed pediatric scaling factors for Hybrid III pediatric ATDs [23][30]. The scale factors and biomechanical response corridors from the TSM have provided a valuable basis for designing and developing ATDs and HBMs, which greatly contributed to improving safety systems. However, the TSM has some limitations: the method inputs of constant density, geometric scaling factors, and elastic modulus were from different portions of the human body

that were not related to the body region of the interest (i.e. scale factors for the pediatric neck responses were based on the scale factors of cranial bone [23] or calcaneal tendon [28][31]). Since there was a lack of biomechanical data in the literature at the time when they developed the TSM, the material properties from the cranial bone and calcaneal tendon had to be utilised. Based on the results from this study, the scaled corridors using TSM, regardless of the age targets (10YO and 15YO), mostly underestimated the pediatric responses, except for head displacement, rotation and lower neck Fx. The assumptions and governing equations used in the TSM may be too simple to generate the pediatric head and neck responses. A complicated, nonlinear analytical approach (e.g. nonlinear governing equations, finite element modeling approach, etc.) may be necessary to develop a better scaling technique for pediatric head and neck responses. In addition, morphological differences in the pediatric cervical spine should be considered in the scaling method. Given the current study only focuses on generating 15YO pediatric head-neck responses and comparing the responses to scaled 10YO and 15YO corridors, efforts to investigate such approaches were not attempted. An extensive set of pediatric biomechanical data for each pediatric demographic would be preferable to avoid relying on any scaling techniques. However, given the sensitive nature of pediatric PMHS research, it is unlikely to have an opportunity to generate such a data set. It is still feasible to enhance current scaling techniques as new pediatric data are added to the literature.

Pediatric head and neck responses

Noticeable phase differences in the pediatric PMHS responses were observed in the head kinematics, upper neck forces, and cervical rotation (Figs 3–4 and Figs B1–B3), likely due to the head lag phenomenon in the pediatric PMHS. The head lag may be induced by inertial differences between the head and neck as well as the flexibility of the pediatric neck. This is evident through the delay in head acceleration in the z-direction followed by a large peak, which suggests that the neck moved with the sled while the head's greater inertia caused it to maintain its original position longer, ultimately delaying acceleration, then reaching a greater peak to compensate. A previous study by Ouyang *et al*. (2005) found that the pediatric cervical spine's bending stiffness and tensile failure loading (no musculature attached in 2–12YO) were less than the adult cervical spine in quasi-static bending and tensile tests [19]. In the current study, the C3 rotation of the pediatric PMHS (-59.6 deg) was comparable to the adult PMHS mean (-57.9 deg), which was the same as the scaled 15YO due to a scale factor of 1.0. However, the C6 rotation from the pediatric PMHS (-42.2 deg) was larger than the adult PMHS (-31.5 deg), indicating that the pediatric PMHS had more pliable joints surrounding C6 than the adult PMHS. The pediatric C3 relative rotation about C6 was lower than the average adult PMHS. This suggests that the pediatric lower cervical spine (C6) was more flexible than the upper cervical spine (C3), contributing to the head lag. This is consistent with previous findings in a pediatric volunteer study by Arbogast *et al*. [26], where they found that the majority of spine flexion occurred at the lower neck. In the Arbogast study, normalised forward head displacement (normalised by sitting height) was greater in the pediatric volunteers compared to adult volunteers tested under the same conditions, indicating the pediatric volunteers had more flexible necks than the adults. The degree of flexion was greater for the youngest pediatric volunteers [26]. Interestingly, they also found that the angle between nasion-external acoustic meatus and C4-T1 was relatively constant with the youngest pediatric volunteers (6–11YO) [23], again demonstrating head inertial properties similar to the response depicted in Fig. B3. Kallieris *et al*. (1976) also found increased head and neck x- and z- displacements compared to those previously observed in adult PMHS [35]. In the Kallieris study, the head lag was described as a delay in neck flexion, which is also consistent with findings from the current study.

The findings from this study, among other biomechanical studies, support the idea that the pediatric lower cervical spine has high pliability. This is supported not only by the biomechanical responses observed in experimental studies but also by epidemiological studies that have shown that higher cervical spine injuries are more common in younger children due to higher fulcrum of motion about the C2/C3 vertebrae [36]. However, a definitive consensus has not been made given the very limited biomechanical and injury responses of the pediatric cervical spine in the existing literature. Lower cervical spine injuries are more common in adults, following full skeletal development, which stiffens the region, increasing the susceptibility of lower neck injury in dynamic environments [13][37]. Some adult PMHS tested in the current study sustained upper thoracic spine damage at T2/T3 due to the large bending moment from the cantilever beam effect. However, the 15YO pediatric PMHS did not sustain any injuries. This could be due in part to the increased pliability of the pediatric neck, which was observed through the kinematic analysis of the vertebrae, in addition to qualitative analysis during the post-test dissection. Collectively, these results demonstrate the need to further pursue the unique biomechanical responses of pediatric cervical spines. Structural and material differences of the pediatric cervical spine contribute

greatly to unique kinematic and kinetic responses that cannot be accurately predicted by scaled adult models alone.

Limitations

Due to extremely limited availability of pediatric PMHS, a single 15YO PMHS was tested in the current study. However, due to the currently available biomechanical responses of the pediatric head and neck in the existing literature, especially in the more severe condition compared to the pediatric volunteer tests [24][26], the 15YO pediatric biomechanical data from the current study provide useful information that can enhance current pediatric ATDs and human body models. Since the 10YO TSM and scale factors were already established and are consistently applied to the current ATDs, the TSM derived 10YO scale factors were first used to evaluate the TSM. The calcaneal tendon stress scale factors from the adult to 10YO were 0.98 [28], which indicated that 10YO material properties referenced in the TSM were similar to adult values (1.0 means same as adult). Therefore, anthropometric parameters from the 10YO were dominating factors for calculating 10YO scale factors in the TSM. The TSM for the 10YO was modified by applying 15YO anthropometric measurements to determine if the anthropometric parameters enhanced the scaling outcomes. However, even when subject-specific scale factors for the 15YO were utilised for TSM, the outcomes from the TSM unsuccessfully replicated the 15YO PMHS head and neck responses. However, differences in material and structural properties between 10YO and 15YO as well as between 15YO and adult PMHS were not considered in this approach. Future work should investigate a new scaling approach that utilises the 15YO and adult PMHS data in this study.

The head mass was measured during post-test dissection but not the head mass moment of inertia (MOI). To calculate an upper neck moment using the inverse dynamic technique, the MOI should be quantified. Given that the C3 relative rotation to the C6 indicated major differences between the pediatric and adult necks, it is important to estimate the head MOI using either the published regression models or CT images. A future study will be conducted to investigate how to quantify MOI accurately so that information regarding the pediatric upper neck moment can be added to the literature.

The lack of muscle activation may exaggerate head and neck kinematics measured from the current PMHS study. It is unknown how the head lag will be reduced by bracing muscles in the frontal impact condition. Computational HBMs could be tuned to match the pediatric responses provided in the current study and use a muscle activation feature to investigate how active muscles affect the head-neck responses.

Although the experimental set-up was repeatable, durable and tightly controlled, it is limited by not simulating whole-body spine kinematics. The T3 was affixed to the load cell, which was directly attached to the mini sled, which accounted for some flexibility of the T1 through T3. Lack of the T3 rotational kinematics could influence lower neck kinematics and kinetics. Since the thoracic spine of the pediatric demographics has been shown to be softer than adult [38], it is important to understand the biomechanical characteristics of the thoracic spine and how the flexibility of the thoracic spine affects the head and neck responses. The effect of the fixed boundary conditions at T3 on the head and neck responses could be also explored using HBMs.

V. CONCLUSIONS

The 15YO pediatric head and neck responses were investigated in a simulated frontal impact condition using a mini sled and comparing responses to scaled biomechanical response corridors. The head lag and large cervical spine rotation were observed in the pediatric responses, which could be explained by the neck pliability of the pediatric neck. The TSM inaccurately produced the scaled pediatric head and neck responses. Due to limited biomechanical data for pediatric PMHS head and neck in frontal impacts, the data from the current study are important to understand the biomechanical characteristics of the pediatric head and neck. The pediatric head and neck responses presented in this study could guide the design of the ATD and HBM necks and enhance their biofidelity.

VI. ACKNOWLEDGMENTS

We are deeply thankful to all the anatomical donors included in this study. We are especially indebted for the opportunity to collect pediatric data, which is critical to advance scientific knowledge and ultimately help protect children from injury. It would not be possible to perform this study without these generous gifts. We would also like to thank students, staff and faculty in the Injury Biomechanics Research Center, specifically Amanda Agnew,

Arianna Willis and Rakshit Ramachandra.

VII. REFERENCES

[1] World Health Organization (2022) “Road traffic injuries” Internet: [https://www.who.int/news-room/fact-sheets/detail/road-traffic-injuries], 20 June 2022 [24 March 2022].

[2] West, B., Rudd, R., Sauber-Schatz, E., Ballestoeros, M, (2021) Unintentional Injury Deaths in Children and Young, 2010-2019. *Journal of Safety Research*, **78**: pp.322–30.

[3] Mohseni, S., Talving, P., *et al*. (2011) Effect of age on cervical spine injury in pediatric population: a National Trauma Data Bank review. *Journal of Pediatric Surgery*, **46**(9): pp.1771–1776.

[4] Leonard, J., Jaffe, D., Kuppermann, N., Olsen, C. (2014) Cervical Spine Injury Patterns in Children. *Pediatrics*, **133**(5): pp.e1179–e1188.

[5] Mallory, A., Stammen, J., Motao, Z. (2019) Cervical and thoracic spine injury in pediatric motor vehicle crash passengers. *Traffic Injury Prevention*, **20**(1): pp.84–92.

[6] Zonfrillo, M., Local, C., Scarfone, S., Arbogast, K. (2014) Motor Vehicle Crash - Related Injury Causation Scenarios for Spinal Injuries in Restrained Children and Adolescents. *Traffic Injury Prevention*, **15**(1): pp.549–555.

[7] Platzer, P., Jaindl, M., *et al*. (2007) Cervical Spine Injuries in Pediatric Patients. *The Journal of Trauma: Injury Infection and Critical Care*, **62**(2): pp.389–396.

[8] Lustrin, E., Karakas, S., *et al*. (2003) Pediatric Cervical Spine: Normal Anatomy, Variants, and Trauma. *RadioGraphics,* **23**(3): pp. 539–801.

[9] Kumaresan, S., Yoganandan, N., Pintar, F., Maiman, D., Kuppa, S. (2000) Biomechanics Study of Pediatric Human Cervical Spine: A Finite Element Approach. *Journal of Biomechanical Engineering*, **122**(1): pp.60–71.

[10] Bailey, D. (1952) The Normal Cervical Spine in Infants and Children. *Radiology*, **59**(5): pp.637–804.

[11] Eleraky, M., Theodore, N., Adams, M., Rekate, H., Sonntag, V. (2000) Pediatric cervical spine injuries: report of 102 cases and review of the literature. *Journal of Neurosurgery*, **92**(1): pp.12–17.

[12] Finch G., Barnes M. (1998) Major Cervical Spine Injuries in Children and Adolescents. *Journal of Pediatric Orthopaedics,* **18**(6): pp.811–814.

[13] Kokoska, E., Keller, M., Rallo, M., Weber, T. (2001) Characteristics of pediatric cervical spine injuries. *Journal of Pediatric Surgery*, **36**(1): pp.100–105.

[14] Kang, Y. S., Stammen, J., Moorhouse, K., Herriott, R., Bolte IV, J. H. (2016) PMHS Lower Neck Load Calculation using Inverse Dynamics with Cervical Spine Kinematics and Neck Mass Properties. *Proceedings of* the International Research Council on Biomechanics of Injury, 2016, pp.143–157..

[15] Kang Y. S., Stammen J., Moorhouse K., Bolte IV, J. H. (2018) Head and Neck Responses of Post Mortem Human Subjects in Frontal, Oblique, Side and Twist Scenarios. Proceedings of the International Research Council on Biomechanics of Injury, 2018, pp.130–149.

[16] Bogduk, N., Yoganandan, N. (2001) Biomechanics of the cervical spine Part 3: minor injuries. *Clinical Biomechanics*, **16**(4): pp.267–275.

[17] Luck, J., Nightingale, R., *et al*. (2013) Tensile Failure Properties of the Perinatal, Neonatal and Pediatric Cadaveric Cervical Spine. *Spine*, **38**(1): pp.E1–E12.

[18] Luck, J., Nightingale, R., *et al*. (2008) Tensile Mechanical Properties of the Perinatal and Pediatric PMHS Osteoligamentous Cervical Spine. *Stapp Car Crash Journal*, **52**: pp.107–134.

[19] Ouyang, J., Zhu, Q., *et al*. (2005) Biomechanics Assessment of the Pediatric Cervical Spine Under Bending and Tensile Loading. *Spine*, **30**(24): pp.E716–E723.

[20] Prasad, P., Danie,l R. (1984) A biomechanics Analysis of Head, Neck, and Torso Injuries to Child Surrogates Due to Sudden Torso Acceleration. *SAE Transactions*, **96**: pp.784–799.

[21] Dibb, A., Cutcliffe, H., *et al*. (2014) Pediatric Head and Neck Dynamics in Frontal Impact: Analysis of Important Mechanical Factors and Proposed Neck Performance Corridors for 6- and 10- Year-Old ATDs. *Traffic Injury Prevention*, **15**(4): pp.386–394.

[22] Wismans, J., Maltha, J., Melvin, J., Stalker, R. (1979) Child Restraint Evaluation by Experimental and Mathematical Simulation. *SAE Transactions*, **88**(4): pp.3455–3474.

[23] Irwin, A., Mertz, H. (1997) Biomechanics Bases for the CRABI and Hybrid III Child Dummies. *SAE Transactions*, **106**(6): pp.3551–3562.

[24] Lopez-Valdes, F., Seacrist, T., *et al*. (2012) A methodology to Estimate the Kinematics of Pediatric Occupants in Frontal Impacts. *Traffic Injury Prevention*, **13**(4): pp.393–401.

[25] Lopez-Valdes, J., Lau, S., Riley, P., Lamp, J., Kent, R. (2011) The Biomechanics of the Pediatric and Adult Human Thoracic Spine. Association for the Advancement of Automotive Medicine, 2011, **55**: pp.193–206.

[26] Arbogast, K., Balasubramanian, S., *et al*. (2009) Comparison of Kinematic Response of the Head and Spine for Children and Adults in Low-Speed Frontal Sled Tests. *Stapp Car Crash Journal*, **53**: pp.329–372.

[27] Pintar, F. A., Yoganandan, N., Maiman, D. J. (2010) Lower cervical spine loading in frontal sled tests using inverse dynamics: potential applications for lower neck injury criteria. Stapp Car Crash Journal, 54: p.133.

[28] Mertz, H., Irwin, A., Prasad, P. (2016) Biomechanics and Scaling Basis for Frontal and Side Impact Injury Assessment Reference Values. *Stapp Car Crash Journal*, **60**: pp.625–657.

[29] Mertz, H.J., Irwin, A.L.,; Melvin, J.W., Stanaker, R.L., Beebe, M.S. (1989). Weight and Biomechanical Impact Response Requirements for Adult Size Small Female and Large Male Dummies. *SAE Technical Paper Series, 1989,* Warrendale, Pa: Society of Automotive Engineers. Paper No. 890756.

[30] Mertz, H. J., Jarrett, K., Moss, S., Salloum, M., Zhao, Y. (2001) The Hybrid III 10 year-old dummy. *Stapp Car Crash Journal*, **45**: pp.319–328.

[31] Melvin, J. W. (1995) Injury Assessment Reference Values for the CRABI 6-month infant dummy in rear-facing infant restraint with airbag deployment. 1995, SAE 950872. Society of Automotive Engineers, Warrendale, PA.

[32] Slykhouse, L., Zaseck, L., *et al*. (2019) Anatomically-based skeletal coordinate systems for use with impact biomechanics data intended for anthropomorphic test device development. *Journal of Biomechanics*, **92**: pp.162–168.

[33] Hagedorn, A., Stammen, J., *et al*. (2022) Biofidelity evaluation of THOR-50M in rear-facing seating configurations using an updated biofidelity ranking system. *SAE International Journal of Transportation Safety*, **10**(09-10-02-0013).

[34] Thunnissen, J., Happee, R., Eummelen, P., Beusenberg, M. (1994) Scaling of adult to child responses applied to the thorax. Proceedings of the International Research Council on Biomechanics of Injury, 1994, pp.229–243.

[35] Kallieris, D., Bars, J., Schmidt, G., Hess, G. (1976) Comparison between child cadavers and child dummy by using child restraint systems in simulated collisions. *Stapp Car Crash Journal*, **20**:5111-542.

[36] Zuckerbraun, B., Morrison, K., Gaines, B., Ford, H., Hackam, D. (2004) Effect of age of cervical spine injuries in children after motor vehicle collisions: effectiveness of restraint devices. *Journal of Pediatric Surgery*, **39**(3): pp.483–486.

[37] Cusick, J., Yoganandan, N. (2002) Biomechanics of the cervical spine 4: major injuries. *Clinical Biomechanics*, **17**(1): pp.1–20.

[38] Sherwood, C., Shaw, C., *et al*. (2003) Prediction of Cervical Spine Injury Risk for the 6-Year-Old Child in Frontal Crashes. *Traffic Injury Prevention*, **4**(3): pp.206–213.

VIII. APPENDIX

Appendix A

TABLE AI
PMHS HEAD AND NECK ANTHROPOMETRY (CM) AND WEIGHT (KG)

	Head Circumference	Head Width	Head Depth	Head Mass	Neck Circumference	Neck Width	Neck Depth	Neck Mass
PED	55.2	13.8	19.1	3.1	34.0	10.7	10.0	1.3
ADT1	56.4	15.5	19.0	3.8	36.5	11.7	10.6	1.4
ADT2	58.0	14.1	19.0	3.6	35.5	12.7	9.2	1.5
ADT3	61.0	15.3	20.3	4.3	43.0	12.7	12.8	1.6
ADT4	57.0	13.5	18.8	3.6	35.5	11.5	8.8	1.4
ADT5	57.6	13.9	19.0	3.7	41.5	11.4	13.5	1.6
ADT50M	58.0	14.5	19.2	3.8	38.4	12.0	11.0	1.5
Mean(SD)	(1.8)	(0.9)	(0.6)	(0.3)	(3.6)	(0.6)	(2.1)	(0.1)

TABLE AII
FILTERING CLASS

		SAE J211 CFC
Head	Acceleration	CFC1000
	ARS	CFC1000
Neck	Force	CFC180
	Moment	CFC180
	Acceleration	CFC180
	ARS	CFC180

Appendix B

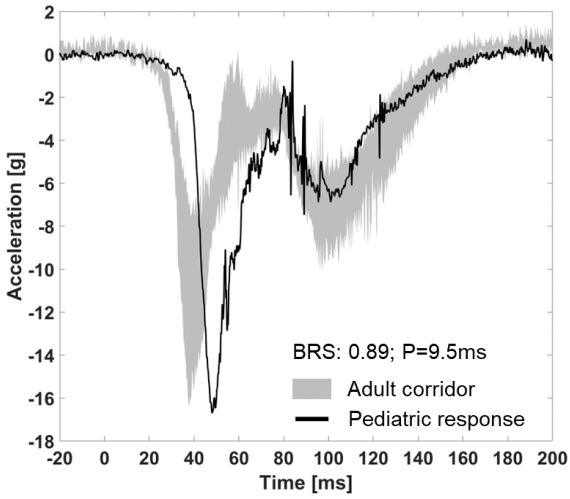

(a) Acceleration in x-direction.

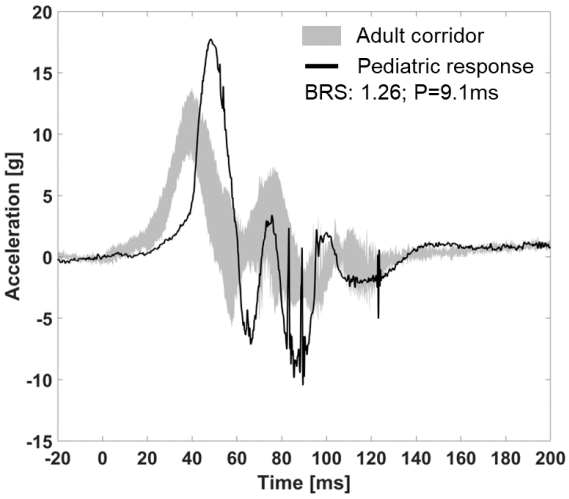

(b) Acceleration in z-direction.

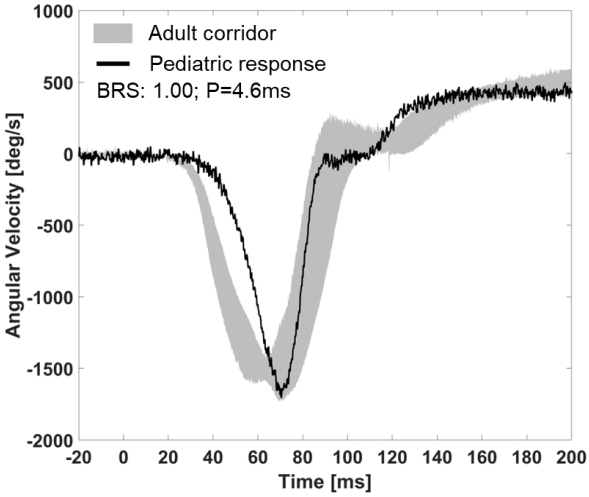

(c) Angular velocity about y-axis.

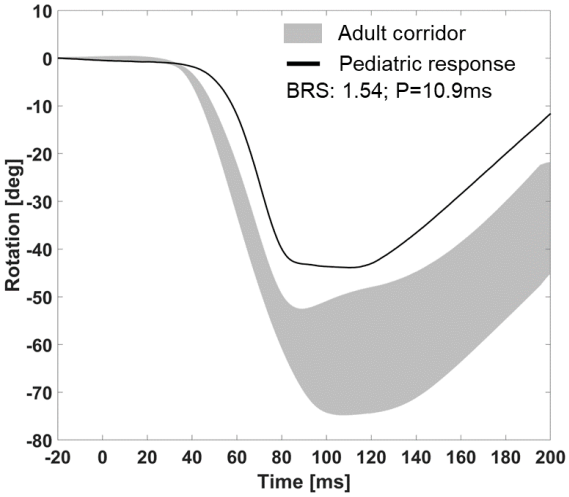

(d) Rotation about Y-axis.

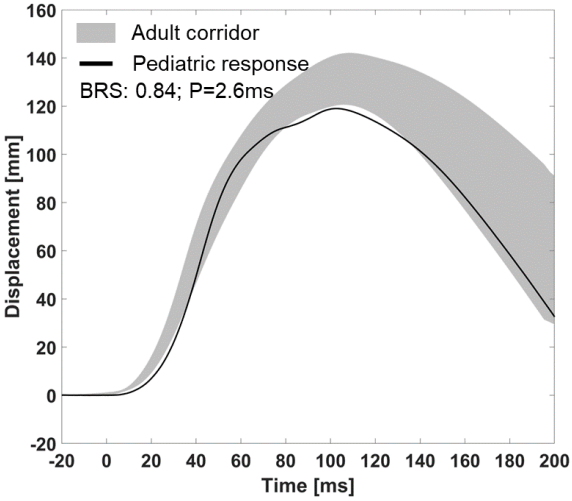

(e) Displacement in sled X-direction.

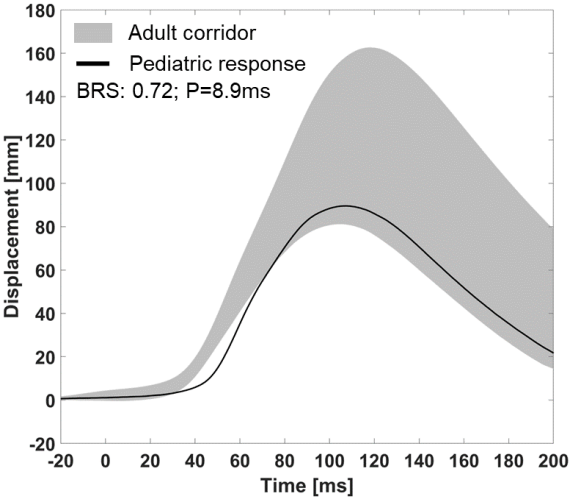

(f) Displacement in sled Z-direction.

Fig. B1. Head kinematics comparison of pediatric PMHS (black) to adult PMHS corridor (gray).

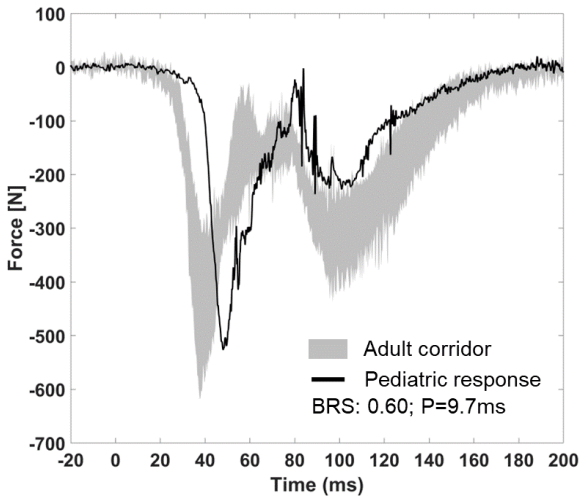

(a) Force in x-direction.

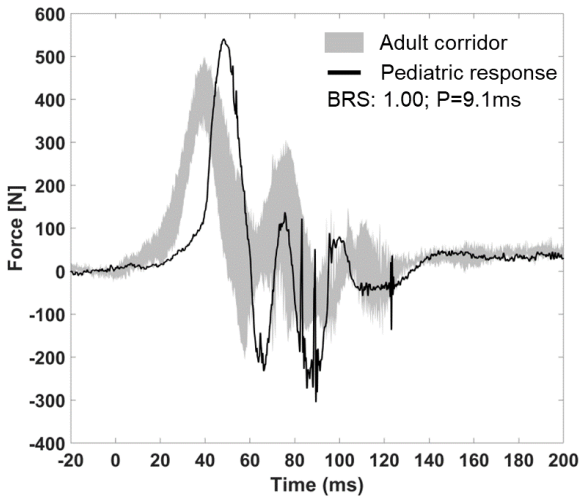

(b) Force in z-direction.

Fig. B2. Upper neck load comparison of pediatric PMHS (black) to adult PMHS corridor (gray).

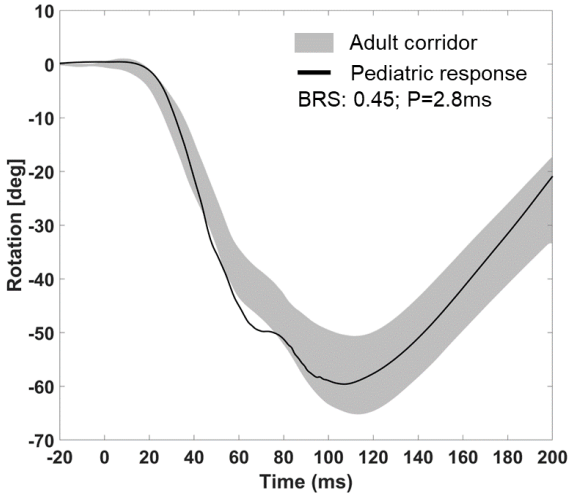

(a) C3 rotation about Y-axis.

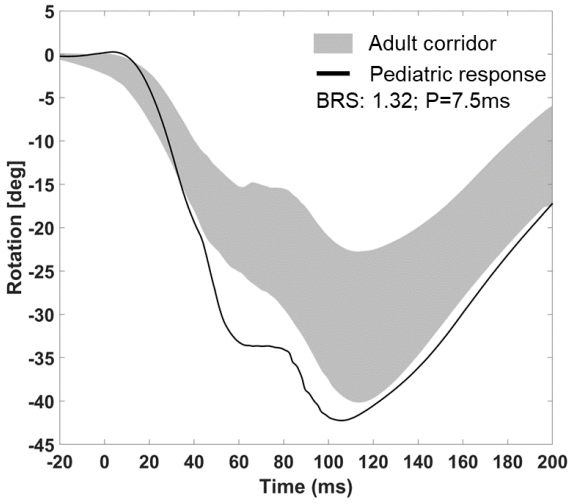

(b) C6 rotation about Y-axis.

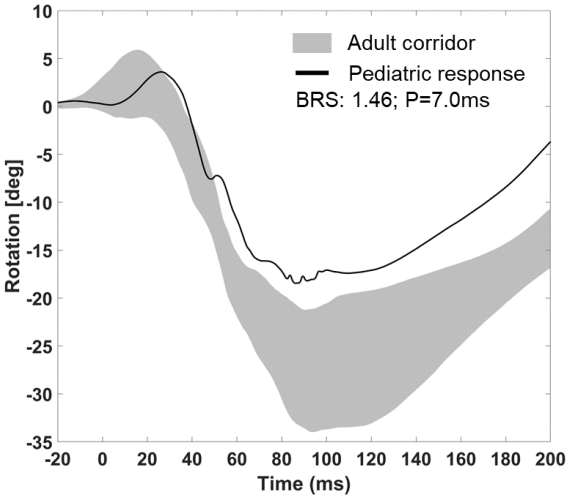

(c) C3 relative rotation to C6 about Y-axis.

Fig. B3. C3 and C6 rotation comparison of pediatric PMHS (black) to adult PMHS corridor (gray).

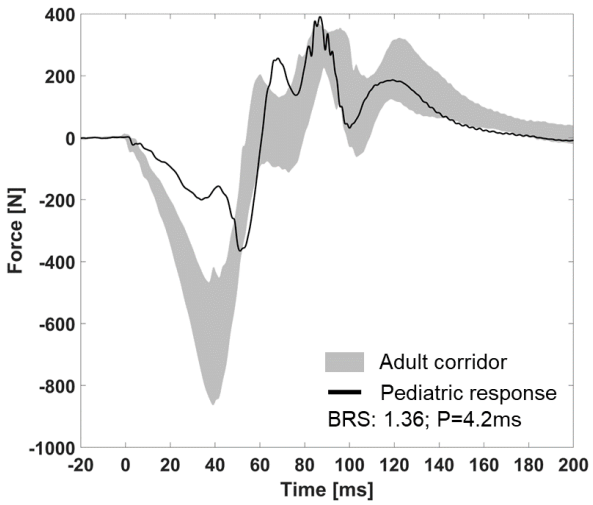

(a) Force in x-direction.

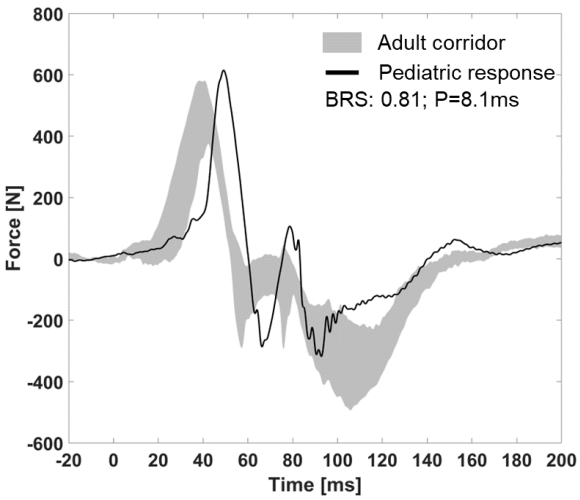

(b) Force in z-direction.

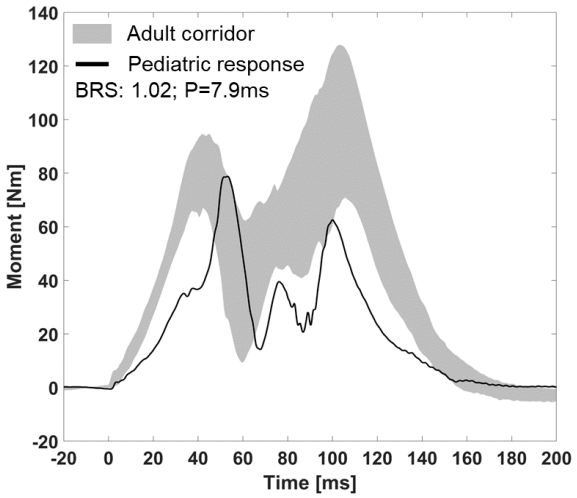

(c) Moment about y-axis.

Fig. B4. Lower neck load comparison of pediatric PMHS (black) to adult PMHS corridor (gray).